The effect of macroscopic field gradients on the simultaneous estimation of reversible and irreversible transverse relaxation rates

Mukund Balasubramanian[1,2] and Robert V. Mulkern[1,2]

[1]*Department of Radiology, Boston Children's Hospital, Boston, MA, United States,* [2]*Harvard Medical School, Boston, MA, United States*

Introduction: Pulse sequences such as GESFIDE[1] and GESSE[2] have enabled the simultaneous measurement of *irreversible* transverse relaxation rates, typically characterized by $R_2=1/T_2$, and *reversible* transverse relaxation rates, typically characterized by $R_2'=1/T_2'$. Reversible relaxation is influenced by both macroscopic and "mesoscopic" field inhomogeneities, with the latter arising from perturbers smaller than the voxel size but larger than the diffusion length[3]. Since increased accumulation of paramagnetic iron substrates such as deoxyhemoglobin, hemosiderin and ferritin leads to increased mesoscopic field variation, extracting this component of the reversible relaxation, by factoring out or correcting for macroscopic effects, is of great importance for characterizing diseased tissue. How best to effect such a correction is, however, not well understood. To investigate this issue, we applied linear macroscopic gradients during GESSE scans of the knee, where significant mesoscopic field inhomogeneities are induced by bone trabeculae. We find that the sinc-term corrections that have been proposed[3,4] are not warranted and that the recently-observed Gaussian behavior of GESSE time-domain signals[5] provides a better avenue for factoring out the effects of macroscopic field variations.

Methods: IRB-approved studies were performed on a Siemens 1.5T Avanto system using a knee receive coil and a 2D multi-slice GESSE implementation with 15 unipolar gradient-echoes at 4.64 ms intervals, with the 8th gradient-echo coinciding with the spin-echo at 80 ms. For each scan, 16 axial slices centered on the left knee of a healthy male volunteer were acquired in ~4 minutes (TR=2s, matrix=128x96), with 5/2.5 mm slice thickness/gap and 2x2 mm^2 in-plane resolution. During each GESSE scan, either no background gradients were applied (BG_0) or a 0.2 mT/m linear gradient was applied in one of three directions: readout (BG_x), phase-encode (BG_y) or slice-select (BG_z). A cylindrical phantom containing $NiSO_4$/NaCl solution was also scanned under similar conditions, to provide a data set where mesoscopic field variations are uniformly close to zero.

Results: Fig. 1 shows, for each background gradient condition, GESSE time courses (logarithm of signal magnitude versus echo time) from 1x1 cm^2 ROIs in bone marrow and muscle. Note that the plots for BG_0, BG_x and BG_y are nearly identical, but very different behavior is seen for BG_z. For bone marrow in the BG_0/BG_x/BG_y condition, signal growth with rate R_2'-R_2 is seen on the left side of the spin-echo and signal decay with rate R_2'+R_2 on the right side, whereas for muscle similar decay is seen on either side due to R_2' being close to zero. The results from the phantom were qualitatively similar to the results in muscle, but with lower R_2 values. In the BG_z condition, signals from muscle and the phantom were well-fit with expressions of the form $S(t) \propto \exp(-R_2(\tau+t))\exp(-(\tau-t)^2\sigma^2/2)$, where τ is the interpulse interval, and 2.35σ is the FWHM of a Gaussian intra-voxel frequency distribution, in line with observations in the brain at 3T[5]. Bone marrow signals are well-characterized by similar expressions, but with an additional R_2' term, i.e., $S(t) \propto \exp(-R_2(\tau+t))\exp(-R_2'|\tau-t|)\exp(-(\tau-t)^2\sigma^2/2)$. If the Gaussian term results from the interaction between non-ideal (e.g., bell-shaped) slice profiles and through-plane gradients[6], the effect of these gradients could be eliminated (or at least significantly reduced) by factoring out this term.

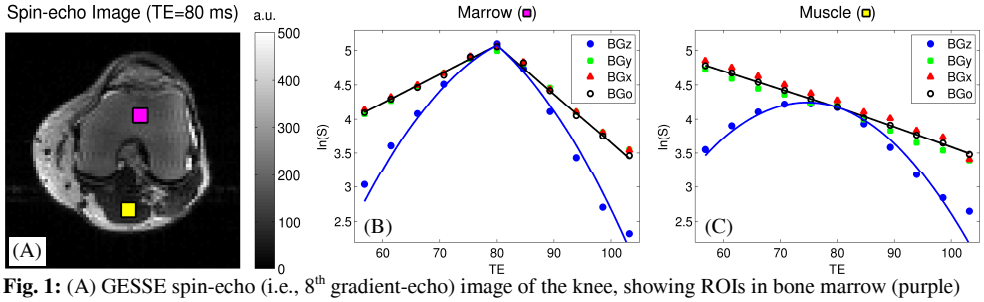

Fig. 1: (A) GESSE spin-echo (i.e., 8th gradient-echo) image of the knee, showing ROIs in bone marrow (purple) and muscle (yellow). GESSE time courses are shown in (B) marrow and (C) muscle with zero gradients (BG_0) or 0.2 mT/m linear gradients applied in the slice-select (BG_z), phase-encode (BG_y) or readout (BG_x) directions.

Fig. 2A and B show R_2' maps for the BG_0 and BG_z conditions, respectively, obtained by fitting exponentials to GESSE time courses[2,5]. Without any attempt to correct for macroscopic field variations, the R_2' map for BG_z (Fig. 2B) is inevitably compromised. A corrected R_2' map (Fig. 2C) was obtained by dividing out the Gaussian term prior to exponential fitting, with σ set to 70 Hz—a value chosen based on fits to the phantom data in the BG_z condition. Fig. 3 shows BG_0 R_2' values plotted against uncorrected BG_z R_2' (red dots), with a root-mean-square difference (RMSD) of 35.1 Hz. Applying the correction described above lowers the RMSD to 9.9 Hz (blue dots).

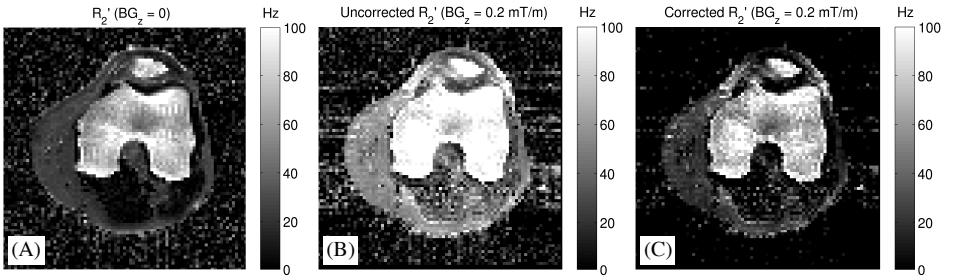

Fig. 2: R_2' maps for the (A) BG_0 and (B) BG_z conditions, showing inflation of R_2' estimates due to the effect of macroscopic gradients in the slice-select direction. (C) R_2' map for the BG_z condition after correction for this effect by factoring out the Gaussian term in the GESSE time-domain signal (see text for details).

Discussion: Our results argue against sinc-term corrections for macroscopic gradients in the slice-select direction (contrary to refs. 3,4) and against the need for any correction for gradients in the readout or phase-encode directions (contrary to ref. 4), and are supported by simulations based on Bloch equation analyses. Good results were obtained via Gaussian corrections for field variations in the slice-select direction, with further improvements envisioned through the use of more sophisticated techniques than the division operation used here, which can lead to noise amplification where the signal is low. Although the background gradients were known a priori here, this will not be the case in general. However, these gradients can be measured via field map acquisitions or perhaps more simply from the phase of the GESSE data itself, thereby allowing σ to be chosen appropriately on a per-voxel basis. While we focused on the knee here because it contains tissues with well-known mesoscopic structure, our results are applicable to the characterization of the mesoscopic structure of a wide variety of tissues, including those in the brain, where assessment of iron deposition and oxygenation status is of paramount importance.

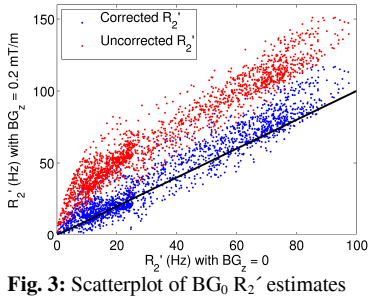

Fig. 3: Scatterplot of BG_0 R_2' estimates vs. uncorrected (red) and corrected (blue) BG_z R_2' estimates.

References: [**1**] Ma J, Wehrli FW. *J Magn Reson B* 1996;111:61-69. [**2**] Yablonskiy DA, Haacke EM. *Magn Reson Med* 1997;37:872-76. [**3**] Fernández-Seara MA, Wehrli FW. *Magn Reson Med* 2000;44:358-66. [**4**] Sedlacik J, Boelmans K, et al. *NeuroImage* 2014;84:1032-41. [**5**] Mulkern RV, Balasubramanian M, Mitsouras D. *Magn Reson Med* 2014;doi:10.1002/mrm.25365. [**6**] Hernando D, Vigen KK, et al. *Magn Reson Med* 2012;68:830-40.